ECS Transactions, 3 (26) 23-29 (2007)
10.1149/1.2753277, copyright The Electrochemical Society

Smart Nanoporous Membranes

S. Smirnov[a]*, I. Vlassiouk[a], F. Rios[a], P. Takmakov[a], D. Gust[b]

[a] Department of Chemistry and Biochemistry, New Mexico State University, Las Cruces, NM 88003, USA
[b] Department of Chemistry and Biochemistry, Arizona State University, Tempe, AZ 85287, USA

The ability to control ion current flow through membranes is important from the fundamental point of view and potentially has a broad range of practical applications including bichemical sensors. In this article we review our results on studying various response mechanisms (such as absorption, fluorescence, electrical conductance) in nanoporous alumina membranes modified with molecular monolayers that are responsive to different physical and chemical stimuli such as light, pressure, and analyte binding.

Introduction

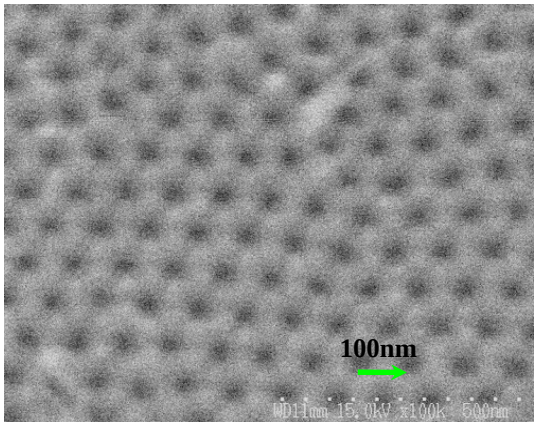

Figure 1. Homemade alumina membrane prepared by anodizing at 40 V in 3% oxalic acid

Alumina nanoporous membranes provide a convenient template for membrane and sensor applications. They can be easily prepared by anodization of aluminum allowing construction of nanoporous membranes with diameters from a few nanometers to several hundreds of nanometes and depths beyond 100 μm (1-2). An example of a homemade membrane prepared in 4% oxalic acid at 40V is given in Figure 1. Commercial membranes (of a lesser quality of pore diameter distribution) are also available from Whatman.

High porosity, small pore diameter comparable with Debye length or/and molecular size, and relatively good optical and IR transparency, have been demonstrated as useful features in constructing sensors, some realizations of which will be demonstrated here.

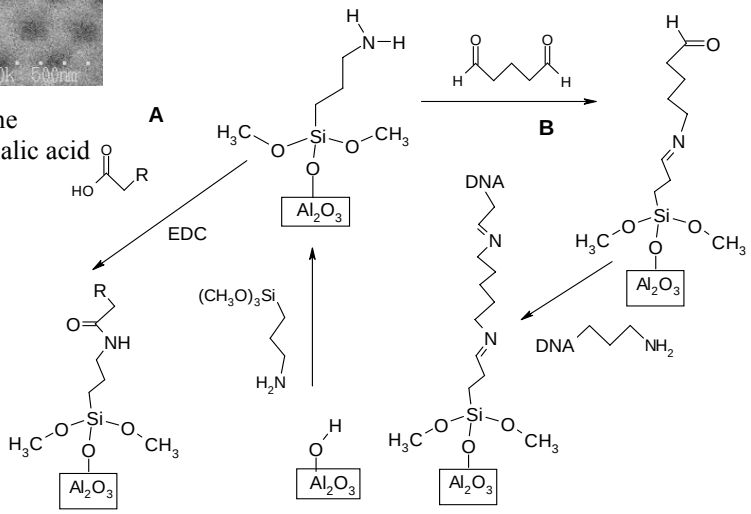

Figure 2. Typical schemes for immobilization of carboxyl (A) and amine (B) terminated molecules on the surface of oxides. Both start by amination with aminoalkoxysilane followed by either (A) amide formation using EDC coupler or (B) activation with gluteraldehyde and reaction with another amine.

Experimental

To make a sensor out of a nanoporous membrane, one needs to modify its surface by molecules that can bind the analytes. It can be either DNA or PNA for sensing nucleic acids of interest (DNA or RNA) or an antigen to capture antibodies (or vice versa). Such surface modification can be achieved in a number of ways. The two most common ones that we use (3-8) are shown in Figure 2. We employ aminoalkoxysilane as a first step to aminate hydroxyl groups on the surface of oxide. It is followed by either EDC (N-(3-dimethylaminopropyl)-N`-ethyl-carbodiimide) promoted coupling with a carboxylic group on a desired molecule or gluteraldehide activation to react with amino group of a molecule such as DNA. We have tried other procedures reported in the literature but found these two the most reliable.

Optical and IR detection

Alumina membranes have a good transparency in the visible range, especially when they are wet but they can be employed for optical detection even in the UV and IR regions. For example, at 260 nm (the maximum absorption wavelength of unmodified DNA) the optical density of commercial membrane from Whatman is below 2, which provides up to 2 units of the dynamic range in absorbance measurements from immobilized molecules. Because of the long (60 μm) and narrow (~200nm) pores, the effective surface is increased by a factor ~ 10^3, which is sufficient for easy detection of even short DNA strands (3). Figure 3 demonstrates UV and IR absorption spectra of immobilized 21-mer long DNA strand on commercial membrane before and after hybridizing with complementary target DNA strand (21-mer for UV and 41-mer for IR). In both cases no tagging of DNA was necessary. The clearly seen increase in absorption reduces back to the original value after denaturing with urea. The process can be repeated numerous times without significant loss of single-stranded DNA covalently bound to the surface, as illustrated by the inset. Denaturing can also be achieved by heating DNA duplex above the melting temperature. The latter for surface bound DNA is very close to the melting temperature measured in solution. Note that the IR spectrum is limited by the transparency window above 1500 cm^{-1}. Lower frequency vibrations are masked by the absorption and scattering by the alumina membrane but absorption due to hydrogen proton, carbonyl, carboxyl, amide and ring stretching near 1600-1700 cm^{-1} are easily observed and can be quantified in sensor applications.

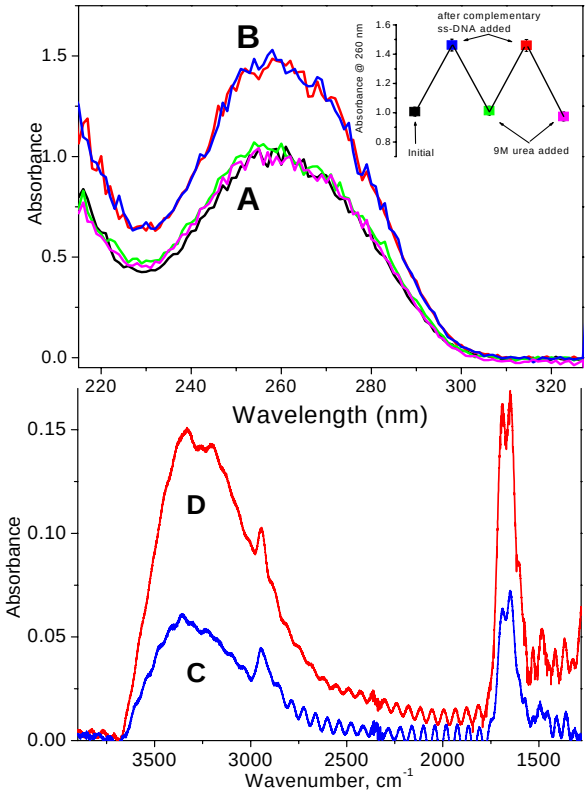

Figure 3. Variation of UV and IR absorption from DNA immobilized inside commercial membranes before (A and C) and after (B and D) hybridization with complementary strand. The inset demonstrates reproducibility

These modified membranes can be also employed as affinity filters to capture single stranded DNA with a desired sequence from the solution that is passed through. We have shown (3) that the complementary sequence can be captured with close to 85 % efficiency from just a single passage.

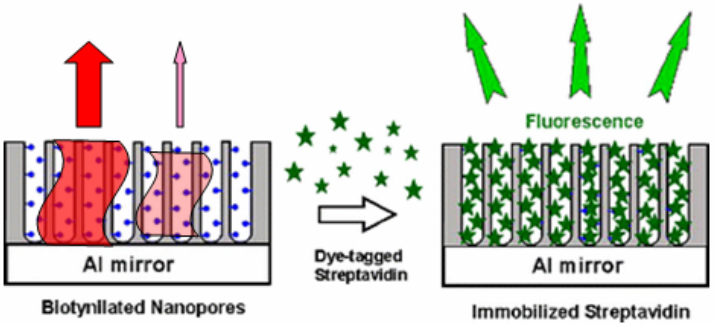

Figure 4. Illustration of fluorescence enhancement arising from increased optical passlength and reflection from underlying Al mirror

High cross-section density of molecules on the surface due to long nanopores can be similarly advantageous in fluorescence based sensors used in biochips and DNA chips (7). It can be further improved and simplified at the same time by leaving the anodized membrane on the Al substrate and by taking advantage of its mirror-like reflection. We have shown that a significant signal increase can be obtained but there are also additional effects arising from optical interference in the resulting dielectric layer (7,9). Proper care should be taken to this interference to maximize the signal: both absorption and fluorescence wavelength regions should be optimized (9).

Electrical detection schemes

For human free analysis, any signal should eventually be transformed into an electrical signal. Thus it would be convenient to bypass all intermediates and design an electrical detection scheme. A very promising and popular realization of such a scheme is based on the field or charge effect, where binding of charged analytes to the surface of one or two dimensional semiconductors depletes the conductive region of charge carriers and thus alter its electrical resistance (10).

We have been exploring an alternative approach, where ionic (rather than electronic) conductance is altered through a single or multiple nanopores as a result of specific analyte binding. Ultimately, one would favor the simplest detection scheme with either DC or AC conductance measurements, preferably with no gating or reference potential (*i.e.* no potentiostat). In the AC mode, it is advantageous to have purely resistive impedance because then simultaneous (parallel) detection of multiple analytes in the same sample can be easily realized.

We identified at least four different mechanisms for altering ionic conductance through the pores each of which can be utilized in sensors, as illustrated in Figure 5.

A. The volume exclusion mechanism is suitable for analytes whose sizes are comparable with the nanopore diameter. The condition is difficult to realize but the advantage is that the method can be used at various ionic strengths. At low ionic strengths the outcome can interfere with the surface charge mechanism - only at high ionic strengths does the signal not depend on the analyte charge.

B. The surface charge mechanism conceptually is very similar to the field effect in electrical conductance (10) but in reverse - with depletion of the ionic carriers inside the nanopore. The effect is pronounced at low ionic strengths (11), when the surface charge with density σ is compensated by the electrolyte with concentration [C]:

$$\sigma/D_{pore} \geq [C]/4, \quad [1]$$

Even for modest surface charge densities, $\sigma \sim 0.01$ e/nm^2, and relatively large pore diameter, $D_{pore} \sim 200$ nm, condition [1] can be achieved at concentrations $[C] \sim 3\times10^{-4}$ M, for which Debye length (12):

$$\lambda_D = 0.307/[C]^{1/2}, \quad [2]$$

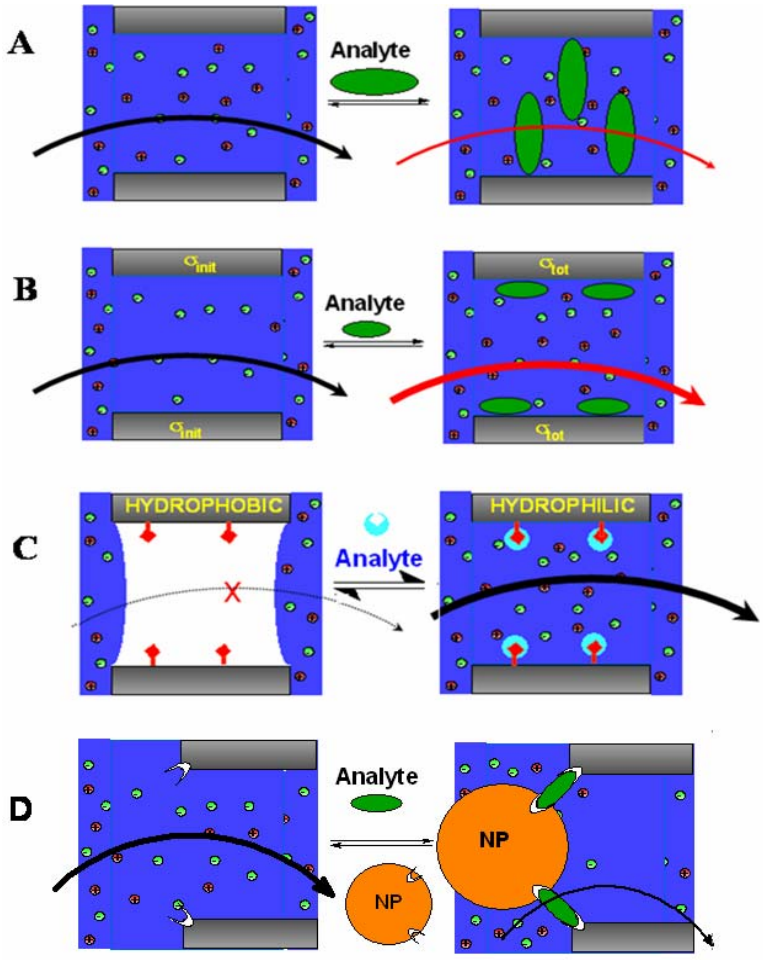

Figure 5. Four mechanisms affecting the ionic conductance through nanopores: **A.** Volume exclusion by bound analytes hinders ionic current. **B**. At low ionic strengths surface charge from bound analytes depletes the nanopore of ions of the same charge; can either increase or decrease the conductance depending on the total change of σ. **C**. Surface tension difference between water and originally dry hydrophobic surface can be decreased by specific binding of hydrophilic analytes, thus allowing electrolyte penetration and electrical shortening of the gap. **D**. Analyte molecules bind nanopoarticles (NP) to the pore mouth to block the pore.

is noticeably smaller than the pore diameter, $\lambda_D \sim 20$ nm. Because of a low ionic strength needed to achieve this condition, where resistance of the pores, R_{pore}, stays constant while that of the electrolyte outside the pore, $R_{electrolyte}$, declines, it becomes more difficult to maintain the former above the latter. The condition $R_{pore} > R_{electrolyte}$ is easier to accomplish with a long single nanopore rather than with multiple short nanopores in parallel, as in nanoporous membranes.

The sign of the effect depends on the change of the total surface charge density (11) and can appear as either increase or decrease of nanopore resistance induced by binding of the analyte.

C. A most dramatic change in the ionic resistance of a nanopore is observed when the surface tension difference between water and the pore surface, $\Delta\gamma$, alters due to physical stimuli or analyte binding and switches it from a hydrophobic and dry to a hydrophilic nanopore (13-14). This hydrophobicity switch allows water to intrude into the pore. It happens near the condition when the contact angle drops from that greater than 90^o (hydrophobic surface) to less than 90^o (hydrophilic surface). The resistance ratio between hydrophobic to hydrophilic membranes can exceed seven orders of magnitude

and thus is very promising, but many details are still not well understood and require additional research.

D. A very naïve approach of blocking nanopores by nanoparticles of appropriate size is no better than the volume exclusion mechanism A and it is definitely less convenient. Figure 6 illustrates that such blocking can be achieved but the main problem is that the fitting is never perfect, especially is one needs it to be discriminative and thus based on a specific interaction induced by analyte. The resulting contrast in resistance is small.

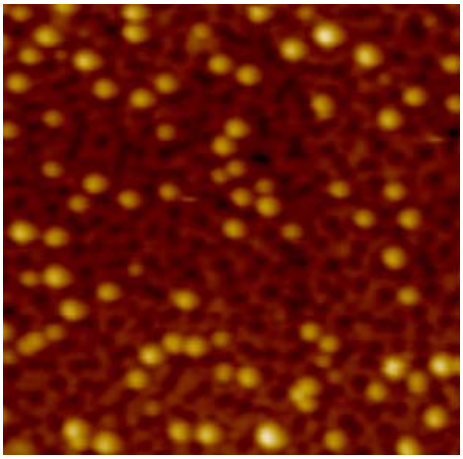

Figure 6. AFM image nonporous membrane partially blocked by silica nanoparticles.

As it follows from the above descriptions, nanoporous membranes are better suited for mechanisms A and C, which have been studied in some details.

The volume exclusion mechanism was demonstrated on sensing DNA in two schemes. First, we employed redox species (ferrocyanine and ruthenium hexamine) to monitor change in their conductance through membrane detected by cyclic voltametry at a noble electrode (4). Conductance (and the corresponding CV amplitude) decrease when surface bound single stranded DNA is hybridized with a complementary strand (see Figure 7) but no changes are observed with a noncomplementary strand that does not hybridize. The effect is only observed on the 20 nm side of the membrane and not on the 200 nm side. The effect is confirmed (4) as due to volume exclusion because it does not depend on the ion charge (is the same for negatively charged ferrocyanine as for positively charged $Ru(NH_3)_6^{2+/3+}$) or ionic strengths (it persists beyond 1.0 M of electrolyte). However, it does depend strongly on the density of surface immobilized DNA, which is expected. redox species and noble electrodes minimize the charge transfer resistance and emphasize contribution from the conductance through the pores. Alternatively, increasing the pore resistance by narrowing the pore diameter lifts the need for low charge transfer resistance. We demonstrated (8) a convenient approach to narrowing alumina pores by boiling the membranes after anodization. It allows detection of DNA hybridization by measuring the ionic conductance of just the electrolyte (8).

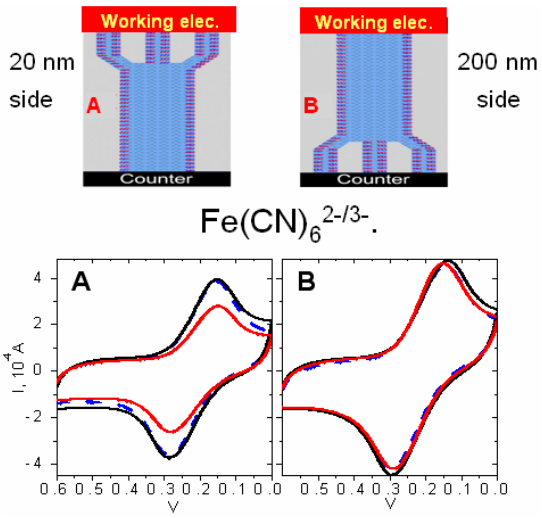

Figure 7. CV of $Fe(CN)_6^{2-/3-}$ at 20 nm (A) and 200 nm (B) side of a nanoporous membrane modified with 21-mer DNA oligomers before and after hybridization with complementary DNA strands.

Hydrophobicity switching requires surface modification with mixed monolayers that consist of both, hydrophobic molecules and 'triggering' molecules that respond to either physical or chemical stimuli (5,14). Optically active spiropyran is less polar in its ground state spiro form but after excitation by UV light transforms into zwitterion (polar) merocyanine that renders the surface more hydrophilic. Irradiation by visible light switches it back to the spiro form. Mixed aliphatic/spiropyran modification of the

membrane surface gradually transforms it from hydrophobic to somewhat hydrophilic upon increasing the portion of spiropyran, but when in the merocyanine (excited) form, this transition occurs at a lower concentration of the dye. In the range of intermediate concentrations one can switch the membrane from its non-conductive dry state to a highly conductive form by means of UV irradiation (5), as shown in Figure 8. Notably, irradiation with visible light that transforms the dye back into its spiro form does not recover the high membrane resistance. The membrane remains filled with water because the dry state is not achievable by spontaneous dewetting for the pore diameters greater than 5 nm due to a high activation barrier. It can be recovered though by membrane drying.

The maximum observed effect in this optical nanovalve as measured via

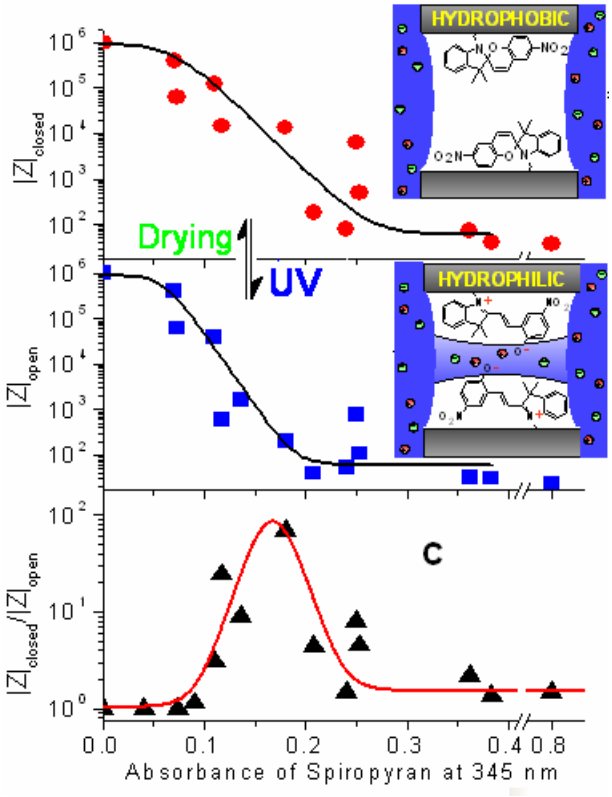

Figure 8. Dependence of the membrane resistance on the relative amount of spiropyran in the hydrophobic monolayer for its (A) spiro (Visible irradiation) and (B) merocyanine (after UV) forms. (C) The effect of light irradiation on the membrane resistance change.

the resistance change (Figure 8C) is partially diminished by the intrinsic *surface wall* conductance of hydrophobic membranes (13), which is sensitive to the type and quality of the organic modifier. The resistance can vary by more than five orders of magnitude even when water does not intrude into the pores and is likely due to surface hydroxyls and other water sensitive/ionizable groups of linkers. Because of that, various hydrophobic modifiers also differentiate membranes by their ability to withstand strong acids, which typically can survive pH < 1 after modification.

Conductance of hydrophobic membranes via surface groups is also observed (14) in studying the pressure dependence of water intrusion into purely

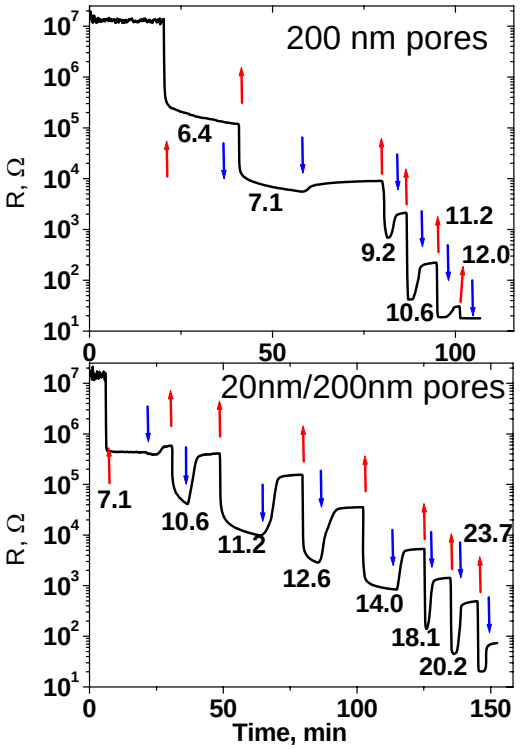

Figure 9. Ionic resistance of nanoporous membranes modified with a fluorinated monolayer as a function of applied pressure. 200 nm diameter pores and 20 nm diameter (on the top of 200 nm) differ not only by the range of pressure intrusion but also by the resistance recovery after releasing pressure.

hydrophobic membranes (Figure 9). The external hydrostatic pressure at which water intrudes into a nanopore depends on its diameter and the surface energy difference between water and the surface:

$$\Delta P = P_{ext} - P_{\text{int}} > \frac{4\Delta\gamma}{D_{pore}} \qquad [3]$$

Commercial '20 nm' membranes have that nominal diameter only on one side and only for ~ 2% of its total thickness; while the remaining part has '200 nm' diameter pores. Compared to one with just 200 nm pores, a 20nm/200nm membrane has a broad range of pressures where its pores are not fully filled with water and thus the activation barrier for dewetting is low. Indeed, a recovery of resistance upon pressure release is observed and it is greater than in '200 nm' membranes but its value is still less than 100%. The effect is important for a proper design of electrical sensors based on the hydrophobicity switching effect, which we believe is the most promising realization of a biochemical sensor.

Thus we demonstrate that nanoporous alumina membranes can be employed in various sensor applications including: optical and IR detection of unlabeled DNA, fluorescence detection of labeled DNA and antibodies, impedimetric (electrical) detection of unlabeled DNA with or without redox pair based on a volume exclusion mechanism. We are developing impedimetric detection schemes for biochemical sensors based on the hydrophobicity switching mechanism and demonstrated enormous changes in the membrane resistances caused by physical and chemical stimuli in such membranes. Electrical conduction by sensitive/ionizable groups underneath the hydrophobic layer on the surface is important for proper design of impedimetric sensors based on hydrophobicity switching.

Acknowledgments

This work was partially supported by a grant from the National Institutes of Health (NIH SCORE GM08136).

References

1. H. Masuda, K. Fukuda, *Science*, **268**, 1466 (1995)
2. A. P. Li, F. Muller, A. Birner, K. Nielsch, U. Gosele, *J. Appl. Phys.* **84**, 6023 (1998)
3. I. Vlassiouk, A. Krasnoslobodtsev, S. Smirnov, M. Germann, *Langmuir*, **20**, 9913 (2004)
4. I. Vlassiouk, P. Takmakov, S. Smirnov, *Langmuir*, **21**, 4776 (2005)
5. I. Vlassiouk, C.-D. Park, S.A. Vail, D. Gust, S. Smirnov, *Nano Letters*, **6**, 1013 (2006)
6. V. Szczepanski, I.Vlassiouk, S.Smirnov, *J. Membr. Sci.*, **281**, 587 (2006)
7. P. Takmakov, I. Vlassiouk, S. Smirnov, *Anal. Bioanal. Chem.*, **385**, 954 (2006)
8. P. Takmakov, I. Vlassiouk and S. Smirnov, *Analyst*, **131**, 1248 (2006)
9. J. Curtiss and S. Smirnov, in preparation
10. F. Patolsky, G. Zheng and C.M. Lieber, Anal. Chem. **78**, 4260 (2006)
11. D. Stein, M. Kruithof, and C. Dekker, *Phys. Rev. Lett.*, **93**, 035901 (2004)
12. A. Bard, L. Faulkner, *Electrochemical Methods. Fundamentals and Applications*. (John Wiley & Sons, 2001).
13. I. Vlassiouk, F. Rios, S. A. Vail, D. Gust, S. Smirnov, *Langmuir*, in press
14. I. Vlassiouk, P.Takmakov, S.Smirnov, *J. Phys. Chem. C*, in press